Available online at www.sciencedirect.com
ScienceDirect
Journal of Solid State Chemistry 180 (2007) 688–694
JOURNAL OF SOLID STATE CHEMISTRY
www.elsevier.com/locate/jssc

On the relaxation/transformation of NiO-dissolved TiO_2 condensates with fluorite-type derived structures

Chang-Ning Huang[a], Pouyan Shen[a], Shuei-Yuan Chen[b,*]

[a]*Institute of Materials Science and Engineering, National Sun Yat-sen University, Kaohsiung, Taiwan*
[b]*Department of Mechanical Engineering, I-Shou University, Kaohsiung, Taiwan*

Received 9 August 2006; received in revised form 2 October 2006; accepted 20 November 2006
Available online 1 December 2006

Abstract

Nd-YAG-laser pulse irradiation of clamped Ni/Ti plates in oxygen was employed to synthesize fluorite-type (f) derived TiO_2 condensates dissolved up to 5 at% Ni^{2+} of the cations. The nanocondensates less than 20 nm in size are nearly cubo-octahedral in shape and tended to transform martensitically to monoclinic (*m*) baddeleyite-type following the crystallographic relationship $(100)_f//(110)_m$; $[001]_f//[001]_m$. The condensates twice larger in size, with considerable matrix constraint, are nearly spherical in shape and consist of mosaic m-twin variants following complicated crystallographic relationships with each other and with the relic *f*-phase: $(010)_f//(\bar{1}\,2\,0)_m$; $[001]_f//[001]_m$. The charge and volume compensating oxygen vacancies due to NiO dissolution in the dense TiO_2 condensates could facilitate the relaxation and amorphization process.

Keywords: TiO_2; NiO dissolution; Fluorite-type; Relaxation; Transformation; Transmission electron microscopy

1. Introduction

Laser pulse irradiation of Ti target in oxygen for a very rapid heating/cooling and nanophase effect has been used to synthesize dense TiO_2 of α-PbO_2-type structure [1], and fluorite-like (denoted as *f*) structure which transformed into monoclinic (*m*-) baddeleyite-type and then α-PbO_2-type structure upon electron irradiation following specific crystallographic relationship depending on the particle size [2].

Here, Nd-YAG-laser pulse irradiation of clamped Ni/Ti plates under oxygen background gas was employed to fabricate NiO-dissolved TiO_2 condensates with baddeleyite-type structure, which behave differently from undoped TiO_2 upon electron dosage. We focused on the effect of NiO dissolution on the specific relaxation/phase transformation path of fluorite-type related TiO_2, which are important in view of the relaxation path of dense dioxides in general [3] and the current discussion of the martensitic transformation of nanosized particles free of matrix constraint [4]. The NiO-dissolved dense TiO_2 condensates with charge/volume compensating defects and being able to transform to *m*-twin variants may have wider photocatalitic applications than undoped TiO_2 [5] and may serve potentially as combined thermal barrier/hard coatings on gas-turbine engine [6] for a beneficial transformation toughening effect analogous to zirconia [7].

2. Experimental

Ni (Nilaco, 99.0% pure, 0.02 mm in thickness) and Ti (Nilaco, 99.5% pure, 0.5 mm in thickness) plates clamped with Ni in the laser incident side were subject to energetic Nd-YAG-laser (Lotis, 1064 nm in wavelength, beam mode: TEM00) pulse irradiation. Oxygen gas (99.999% purity) at a flow rate of 20–50 L/min was supplied to oxidize and cool the condensates inside the ablation chamber. Laser pulse energy 500 and 1100 mJ/pulse, i.e., power density of 7.0×10^7 and 1.5×10^8 W/cm^2, respectively, given pulse time duration of 240 μs at 10 Hz on focused area of 0.03 mm^2, assured a good yield of NiO-dissolved TiO_2 condensates.

*Corresponding author. Fax: +886 7 657 8853.
E-mail address: steven@isu.edu.tw (S.-Y. Chen).

0022-4596/$ - see front matter © 2006 Elsevier Inc. All rights reserved.
doi:10.1016/j.jssc.2006.11.027

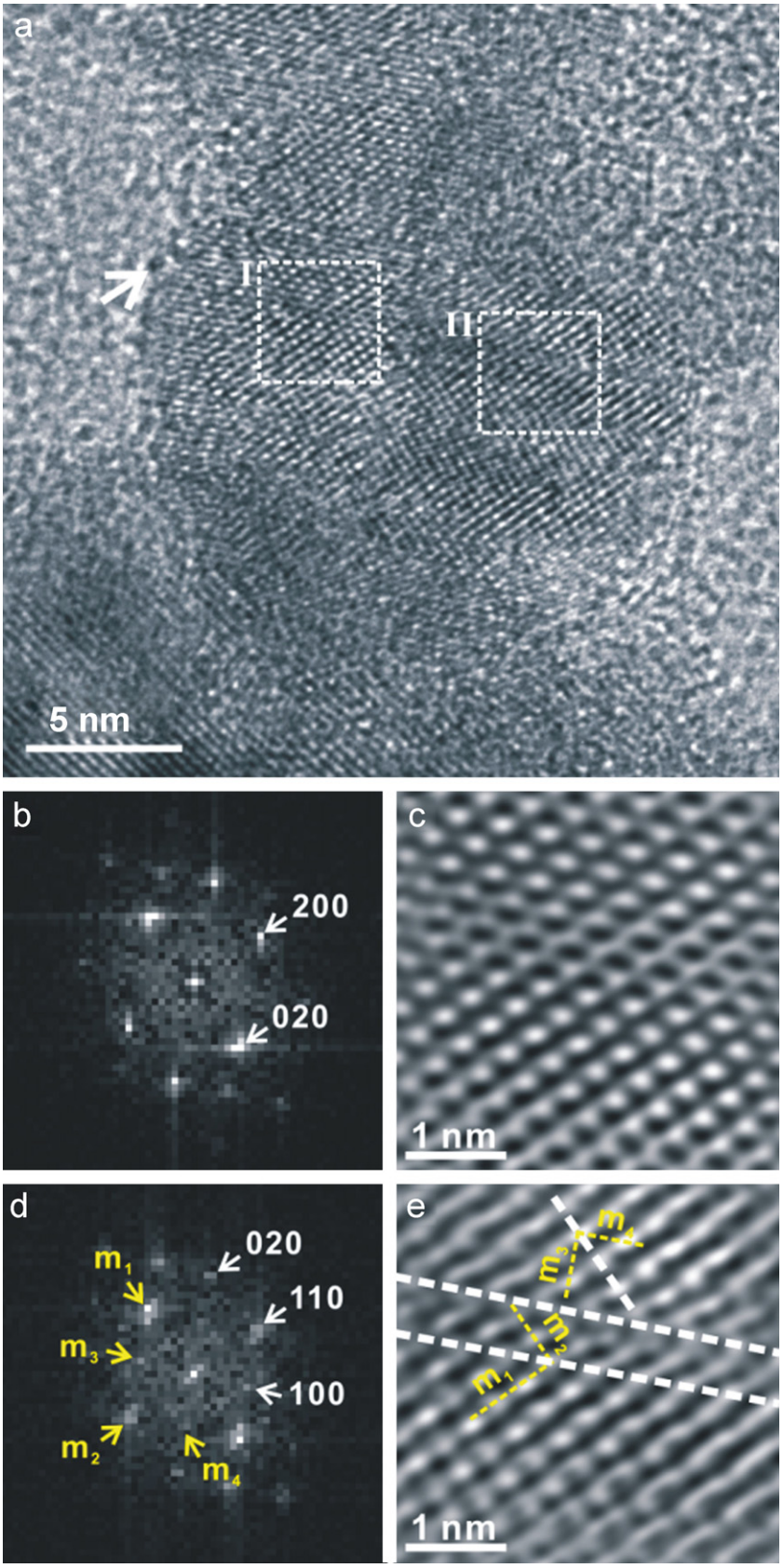

Fig. 1. (a) Lattice image of a nearly cubo-octahedral NiO-dissolved TiO_2 condensate ca. 17 nm in diameter of fluorite (denoted as f) and monoclinic (denoted as m) baddeleyite-type structures having edge-on (010) facet (arrow), (b)/(c) and (d)/(e) are 2-D Fourier transform ([001] zone axis) and inverse Fourier transform from the square region I (*f*-phase) and II (*m*-phase), respectively, in (a). The *m*-twin variants 1–4 are separated by {010} and {110} boundaries (white dashed lines) and the $\{110\}_{m1}$, $\{110\}_{m2}$, $\{100\}_{m3}$ and $\{010\}_{m4}$ planes are denoted by yellow dashed lines in (e).

Copper grids overlaid with a carbon-coated collodion film and fixed in position by a holder at a distance of 2.5–10 mm from the target were used to collect the condensates. The NiO-dissolved TiO_2 condensates were identified by analytical electron microscopy (AEM, JEOL 3010 instrument at 300 keV) having selected area electron diffraction (SAED) pattern taken with 1 μm-diameter aperture, and point-count energy-dispersive X-ray (EDX) analysis at a beam size of 10 nm. Bright field images (BFI) taken by transmission electron microscopy (TEM) were used to study the general morphology and agglomeration of the condensed NiO-dissolved TiO_2 particles. Lattice imaging coupled with 2-D Fourier transform and inverse transform were used to analyze the crystal structure, defects and phase transformation of nano-size particles. (The ring electron diffractions from the condensates covered in a selected area aperture of 1 μm allowed unambiguous determination of the crystal structure of the NiO-dissolved TiO_2 polymorphs. The individual nanoparticles, however, are too small to give SAED pattern and rely on 2-D Fourier transforms of the lattice image for the crystal structure and defect analysis.) The *d*-spacings measured from SAED patterns were used for least-squares refinement of the lattice parameters. The *m*-type structure was indexed according to the distorted version of c-fluorite type parent cell as adopted for zirconia [8]. The cell parameter was determined as 0.4520 ± 0.0005 nm for the NiO-dissolved TiO_2 nanoparticles with fluorite-type structure. The *m*-type structure was distorted from place to place and therefore difficult, if not impossible, to determine the lattice parameters.

3. Results

Electron diffraction and EDX analysis (not shown) indicated the randomly oriented condensates are predominant rutile/anatase with minor *f*- and α-PbO_2-type structure, all dissolved with considerable amount of Ni. A total of 5 independent TEM observations of NiO-dissolved TiO_2 condensates with fluorite-type derived structures were made in this study. The microstructures and transformation behavior typical to relatively small- and large-sized particles are in the following.

The *f*-type NiO-dissolved TiO_2 nanocondensates are typically close to cubo-octahedral in shape having twin boundaries {010} and {110} due to partial transformation to *m*-phase as shown by the lattice image, 2-D Fourier transform and inverse transform in Figs. 1(a)–(c). One of the *m*-variants in this case follows the specific crystallographic relationship $(100)_f//(110)_m$; $[001]_f//[001]_m$, having other $(hkl)_f//(hkl)_m$ pairs nearly in parallel (within 4 degrees) according to the stereographic projection (Fig. 2). After

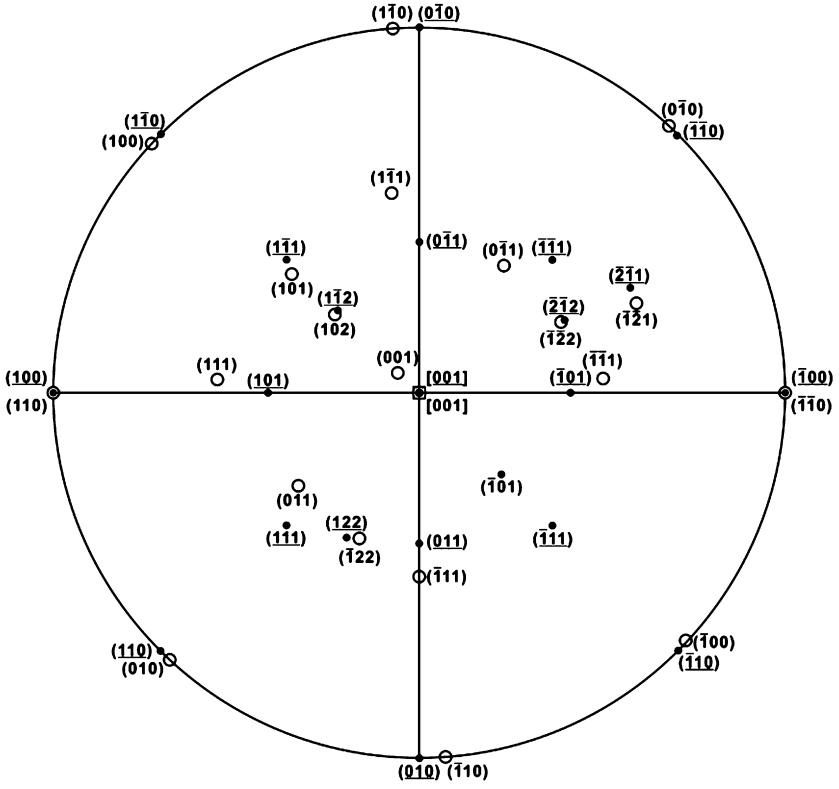

Fig. 2. Stereographic projection of the plane normals (circles) and zone axes (squares) of the parent fluorite-type NiO-dissolved TiO_2 denoted by solid symbols and underlined (*hkl*), and monoclinic baddeleyite-type variants denoted by open symbols with (*hkl*) following the crystallographic relationship $(100)_f//(110)_m$; $[001]_f//[001]_m$. Note superimposed plane normals: $(100)_f//(110)_m$; $(\bar{1}\,0\,0)_f//(\bar{1}\,\bar{1}\,0)_m$, and nearly superimposed plane normals: $(1\,\bar{1}\,0)_f//(100)_m$ (2.05° off), $(\bar{1}\,0\,0)_f//(1\,\bar{1}\,0)_m$ (4.11° off), $(\bar{1}\,\bar{1}\,0)_f//(0\,\bar{1}\,0)_m$ (2.05° off), $(\bar{1}\,1\,0)_f//(\bar{1}\,0\,0)_m$ (2.05° off), $(010)_f//(\bar{1}\,1\,0)_m$ (4.11° off), $(110)_f//(010)_m$ (2.05° off), $(1\,\bar{1}\,2)_f//(102)_m$ (1.19° off), $(1\,\bar{1}\,1)_f//(101)_m$ (3.87° off), $(\bar{2}\,\bar{1}\,2)_f//(\bar{1}\,\bar{2}\,2)_m$ (1.14° off), $(\bar{2}\,\bar{1}\,1)_f//(\bar{1}\,\bar{2}\,1)_m$ (3.67° off) and $(122)_f//(\bar{1}\,2\,2)_m$ (3.26° off).

electron irradiation at a beam current of 60 pA/cm^2 for a total of 60 s, the *f*-type particle in Fig. 1 become amorphous hardly with crystalline relic as indicated by lattice image (Fig. 3(a)) and diffuse diffraction intensity in the 2-D Fourier transform in (Fig. 3(b)). There are abundant dislocations and disordered regions in the transformed particle (Fig. 3(a)), which is dissolved with NiO as indicated by point count EDX analysis (Fig. 3c).

The relatively large condensate of f-phase, ca. 43 nm in diameter, tended to transform into mosaic twin variants of *m*-structure with {010} facets upon quenching to ambient pressure as indicated by lattice image (Fig. 4(a)) and 2-D Fourier transform (Fig. 4(b)). The *m*-phase formed twin variants following the crystallographic relationship $(010)_f//(\bar{1}\,2\,0)_m$; $[001]_f//[001]_m$ with the *f*-phase, the same as that reported for undoped TiO_2 condensates ca. 53 nm in diameter [2]. The *m*-twin variants, however, follow complicated crystallographic relationships among themselves, which are beyond the scope of the present research. The reconstructed image (Fig. 4(c)) shows (010) slip/twin planes of the partially transformed particle. Such relatively large condensates are also vulnerable to electron dosage by transforming into amorphous phase hardly with crystalline relic as indicated by lattice image (Fig. 5(a)) and 2-D Fourier transform (Fig. 5(b)). Point-count EDX analysis (Fig. 5(c)) indicated the transforming particle is again TiO_2 containing dissolved NiO.

4. Discussion

4.1. Assignment and defect chemistry of the NiO-dissolved TiO_2 with fluorite-type related structure

The baddeleyite-type phase in the present condensates has (010) slip/twin planes, indicating it has been martensitic transformed from parental fluorite-type structure. 2-D Fourier transform with corresponding reconstructed image from the local region indeed shows such relic. It is difficult, if not impossible, to determine the space group for the fluorite-like relic because of structure distortion and damage upon electron irradiation. Still the fluorite structure rather than other fcc-type structure, such as Pa

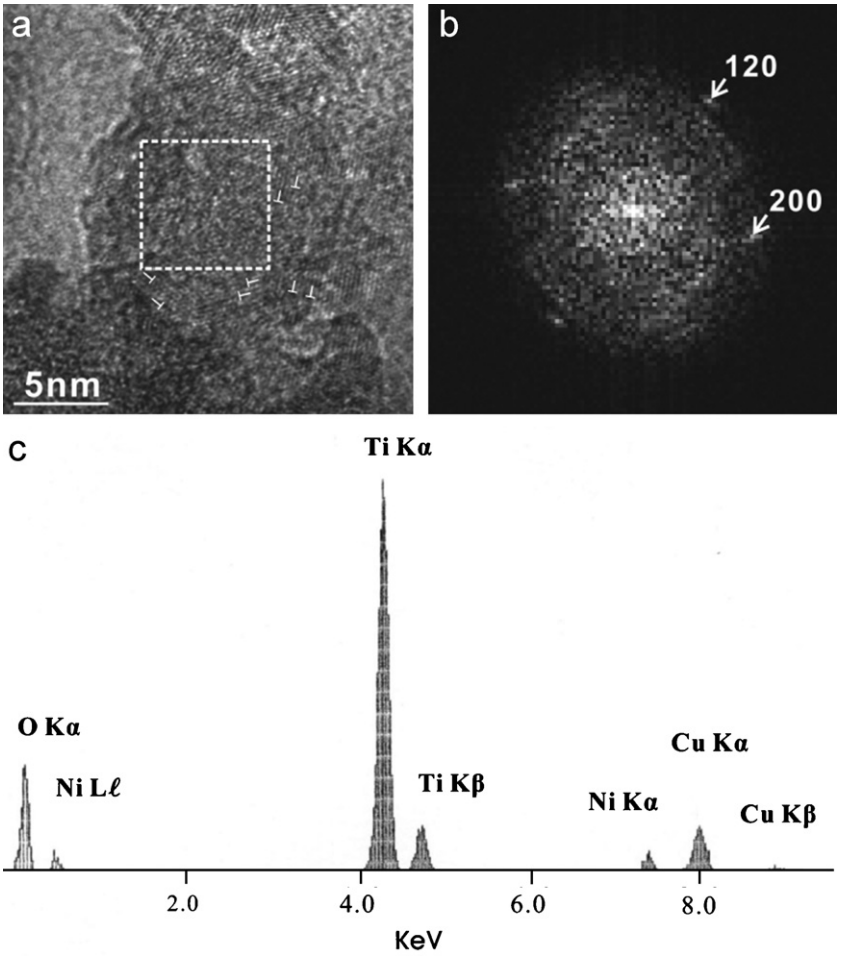

Fig. 3. (a) Poorly crystalline image with abundant dislocations (denoted as T) and disordered regions for the small particle in Fig. 1 after electron irradiation for 60 s to become amorphous hardly with baddeleyite-type relic as indicated by diffuse diffraction intensity in the 2-D Fourier transform in (b). (c) EDX spectrum showing NiO content (3.3 at% Ni) in the transforming particle.

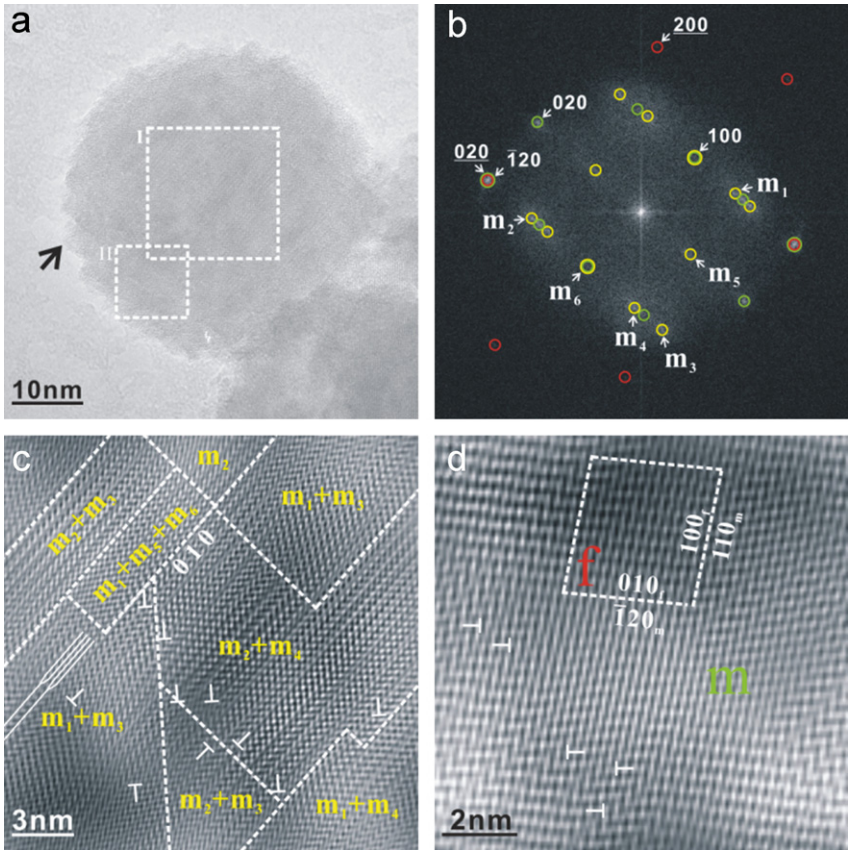

Fig. 4. (a) Transmission electron micrograph (lattice image) of NiO-dissolved monoclinic (m-) baddeleyite-type TiO_2 condensate ca. 43 nm in diameter with {010} facets (indicated by arrow); (b) 2-D Fourier transform ([001] zone axis) of the particle showing diffraction spots of m- (green open circles and *hkl*) and relic fluorite-type (denoted by *f*, red open circles and *hkl*) with a specific lattice correspondence (refer to text), with the twin spots of *m*-variants 1–6 as indicated by yellow open circles; (c) reconstructed image from the square region I showing dislocations (denoted by T) and faults/twin planes of *m*-variants parallel to (010) and/or (110); (d) reconstructed image from the square region II showing distorted *f*-domain with coherent (020) *d*-spacing = 0.227 nm across the $(010)_f/(\bar{1}20)_m$ and $(100)_f/(110)_m$ boundaries.

$\bar{3}$-modified type of the dense SnO_2 [9,10], can be reasonably assigned for the NiO-dissolved TiO_2 based on the following reasons. First, the descendants of baddeleyite-type variants are indicative of a parent fluorite structure rather than pyrite structure, analogous to the case of ZrO_2 [7] and undoped TiO_2 [2]. Second, the observed (010) twinning and deformation scheme is in accord with the martensitic transformation from the fluorite type to the baddeleyite-type structure for the dioxides [2,7]. In any case, the presence of charge and volume compensating oxygen vacancies, through the following defect chemistry considerations, could facilitate relaxation and amorphization of the NiO-dissolved TiO_2 with the fluorite-type-related structures.

The enhanced solid solubility of NiO in the fluorite-type TiO_2 condensates has nothing to do with negligible other impurities, but can be attributed to the effect of pressure as suggested for significantly widened MgO solid solubility in ZnO [11–14] (Wurtzite-type ZnO was reported to have a wider solid solubility of MgO under the influence of hydrostatic pressure [11] or via a laser ablation coating process [12–14]). The defect chemistry of NiO-dissolved dioxide with fluorite-type structure has been addressed for plasma-sprayed yttria-partially stabilized zirconia (Y-PSZ) [15]. By analogy, the defect chemistry equations for the substitution of Ti^{4+} with Ni^{2+} in coordination number (CN) 8 are as follows:

$$NiO_{(s)} \xrightarrow{TiO_2} Ni''_{Ti} + O_o^{\times} + V_o^{\cdot\cdot}.$$

The oxygen vacancies were then introduced as charge compensating defects to maintain electron neutrality and to stabilize the fluorite-type structure analogous to the cases of fully stabilized cubic phase [16] or PSZ of cubic plus tetragonal phases [17]. The $V_O^{\bullet\bullet}$ might induce $Ti_i^{\cdot\cdot\cdot\cdot}$ and/or $Ni_i^{\cdot\cdot}$ for volume compensation. Defect clusters such as $[Ni_{Ti}''-V_O^{\bullet\bullet}]$, $[3\ NiTi''-V_O^{\bullet\bullet}-Ti^{\cdot\cdot\cdot\cdot}]$ and $[2Ni_{Ti}''-V_O^{\bullet\bullet}-Ni_i^{\cdot\cdot}]$ could then form in the fluorite-type structure. It should be noted that the effective ionic radius of Ni^{2+} (0.0690 nm) is larger than Ti^{4+} (0.0605 nm) in CN 6 [18]. The effective ionic radius of Ni^{2+} in CN 8 is not available, but is expected to be larger than Ti^{4+} (0.074 nm) in CN 8. The substitution of Ni^{2+} for Ti^{4+} in CN 8 of fluorite-type structure would then cause a larger lattice parameter and volume compensating oxygen vacancies. On the other hand, residual stress up to ca. 10 GPa level in view of

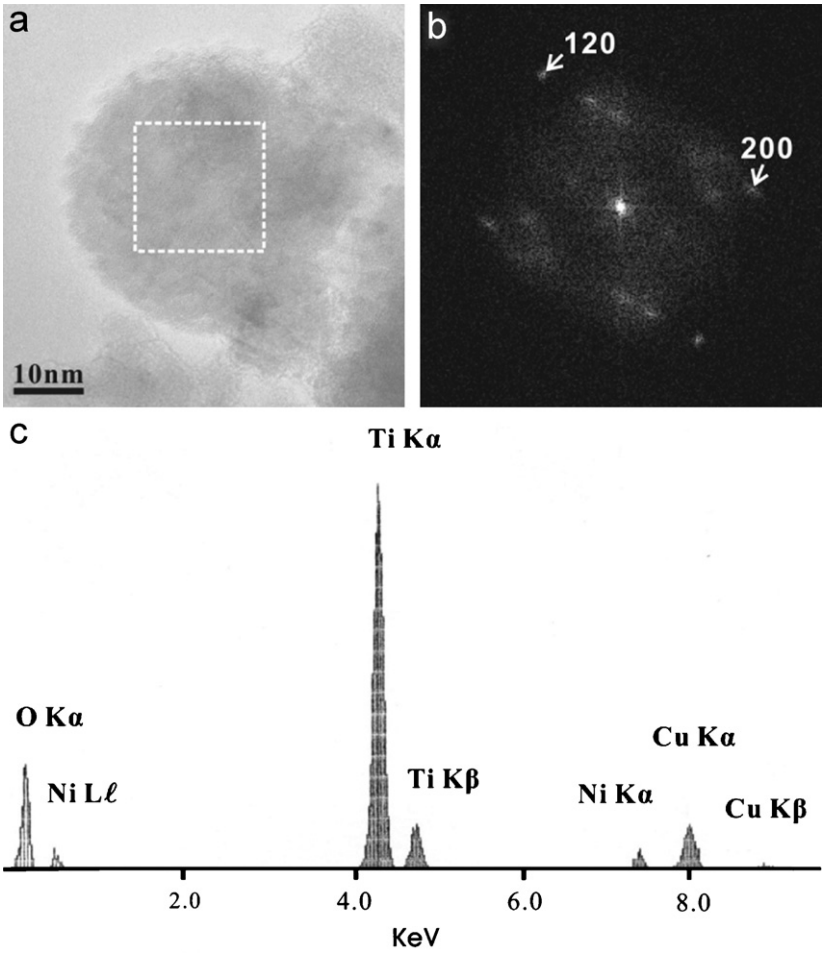

Fig. 5. (a) Lattice image of the particle in Fig. 4 after electron irradiation for 90 s to become amorphous with dimmed diffractions of baddeleyite-type relic as indicated by arrows in the 2-D Fourier transform in (b). (c) EDX spectrum showing significant NiO content (4.9 at% Ni) in the transforming particle.

undoped TiO_2 condensates with dense structures [1,2,19] would compress the unit cell. The two combined effects then caused a lattice parameter of 0.452 nm for the NiO-dissolved TiO_2 with fluorite-type structure, based on its (200) *d*-spacing in the lattice image (Fig. 4). It should be noted that minor Ti^{+3} and/or Ti^{2+} may introduce additional charge compensating oxygen vacancies for the NiO-dissolved TiO_2 to stabilize as the fluorite-type structure analogous to the case of Ti-stabilized zirconia [20].

4.2. Implications

The fluorite-type TiO_2 condensates being dissolved with NiO and transformed martensitically to baddeleyite-type twin variants may have potential applications as a visible-light-responsive photocatalyst as well as thermal barrier/hard TiO_2 coating on Ni-based alloys for a beneficial transformation toughening effect. This prospect is encouraged by theoretical calculations of undoped dense TiO_2 [21,22].

In fact, the first principle calculations of the TiO_2 polymorphs [21] indicated that the fluorite type has the narrowest band gap 1.08 or 2.18 eV after applying a very approximate band gap correction [21]. Thus fluorite-type TiO_2 may have potential applications as a visible-light-responsive photocatalyst as the ambient TiO_2 [5]. The dissolution of NiO component in fluorite-type TiO_2 nanocondensates may have even wider such applications because of charge transfer and tailored band gap imposed by alloying besides the beneficial large surface area of the nanoparticles. It is by no means clear, however, whether the NiO dissolution would improve the light transmittance and the photocatalytic activity of TiO_2 as provoked for $TiO_{2-x}N_x$ films by visible light irradiation [23–25].

As far as the mechanical properties are of concern, the Vickers hardness calculations [22] assuming pseudobinary compound with μ bond separated into covalent gap and ionic gap parts [26] indicated that the dense TiO_2 polymorphs have increasing hardness with the increase of density, i.e., 30, 32, 33 and 35 GPa for α-PbO_2-, baddeleyite-, fluorite- and cotunnite-type, respectively. The predicted hardness agrees within 10% of the experimental value (38 GPa) for cotunnite-type TiO_2, the hardest oxide known [27]. Having a theoretical high hardness and additional transformation toughening effect analogous to

martensitic transformation of PSZ [7], tetragonal zirconia polycrystals nanometer in grain size [28], and epitaxial nanocrystalline material of zirconia on NaCl [29], the NiO-dissolved TiO_2 condensates with fluorite-type structure may have potential hard coating applications on nickel-based superalloys in gas turbine engine [6]. The free nanocondensates of NiO-dissolved TiO_2 immune from any precipitates in the fluorite-type structure would undergo martensitic transformation like the isolated zirconia nanoparticles upon irradiation or stress [4]. Whereas, such nanocondensates when coalesced/accumulated as a thin coating on suitable substrates would behave like nanocrystalline layer material [29] for a more efficient transformation toughening effect. Thus for the sake of potential applications, it is worthwhile to explore laser ablation condensation at a higher power density for a very rapid heating/cooling and hence pressure effect [1] on the stabilization of the dense condensates with fluorite-type-related structures.

5. Conclusions

(1) Fluorite-type derived TiO_2 condensates dissolved with nearly 5 at% Ni were synthesized by energetic pulse laser ablation on Ni/Ti composite target in oxygen.
(2) The fluorite-type (*f*) nanocondensates are nearly cubo-octahedral in shape and tended to transform martensitically to monoclinic (*m*) baddeleyite-type following the crystallographic relationship $(100)_f//(110)_m$; $[001]_f//[001]_m$.
(3) The larger condensates with considerable matrix constraint, are nearly spherical in shape and consist of mosaic *m*-twin variants following complicated crystallographic relationships with each other and with the relic *f*-phase: $(100)_f//(\bar{1}\,2\,0)_m$; $[001]_f//[001]_m$.
(4) The charge and volume compensating oxygen vacancies due to NiO dissolution in the dense TiO_2 condensates could facilitate the relaxation and amorphization process.

Acknowledgments

We thank anonymous referees for constructive comments. This research is supported by Center for Nanoscience and Nanotechnology at NSYSU and National Science Council, Taiwan, ROC under contract NSC94-2120-M110-001.

References

[1] S.Y. Chen, P. Shen, Phys. Rev. Lett. 89 (2002) 096106-1.
[2] S.Y. Chen, P. Shen, Jpn. J. Appl. Phys. 43 (2004) 1519.
[3] B.G. Hyde, L.A. Bursill, M. O'Keeffe, S. Andersson, Nat. Phys. Sci. 237 (1972) 35.
[4] P. Shen, W.H. Lee, Nano Letters 1 (2001) 707.
[5] A.L. Linsebigler, G. Lu, J.T. Yates Jr., Chem. Rev. 95 (1995) 735.
[6] N.P. Padture, M. Gell, E.H. Jordan, Science 296 (2002) 280.
[7] D.J. Green, R.H.J. Hannink, M.V. Swain, Transformation Toughening of Ceramics, CRC Press, Boca Raton, FL, 1989.
[8] G. Teufer, Acta Crystallogr. 15 (1962) 1187.
[9] J. Haines, J.M. Léger, Phys. Rev. B 55 (1997) 11144.
[10] J. Haines, J.M. Léger, O. Schulte, Science 271 (1996) 629.
[11] M. Kunisu, I. Tanaka, T. Yamamoto, T. Suga, T. Mizoguchi, J. Phys.: Condens. Matter 16 (2004) 3801.
[12] A. Ohtomo, M. Kawasaki, T. Koida, K. Masubuchi, H. Koinuma, Y. Sakurai, Y. Yoshida, T. Yasuda, Y. Segawa, Appl. Phys. Lett. 72 (1998) 2466.
[13] S. Choopun, R.D. Vispute, W. Yang, R.P. Sharma, T. Venkatesan, Appl. Phys. Lett. 80 (2002) 1529.
[14] P. Bhattacharya, R.R. Das, R.S. Katiyar, Appl. Phys. Lett. 83 (2003) 2010.
[15] S. Chen, P. Shen, Mater. Sci. Eng. A 114 (1989) 159.
[16] S. Fabris, A.T. Paxton, M.W. Finnis, Acta Mater. 50 (2002) 5171.
[17] A.H. Heuer, M. Rühle, in: A.H. Heuer, L.W. Hobbs (Eds.), Science and Technology of Zirconia II. Advance in Ceramics, vol. 12. The American Ceramic Society, Columbus, OH, 1984.
[18] R.D. Shannon, Acta Crystallogr. A 32 (1976) 751.
[19] M.H. Tsai, Ph.D. Thesis, National Sun Yat-sen University, Taiwan, 2004.
[20] C.L. Lin, D. Gan, P. Shen, J. Am. Ceram. Soc. 71 (8) (1988) 624.
[21] M.Y. Kuo, C.L. Chen, C.Y. Hua, H.C. Yang, P. Shen, J. Phys. Chem. B 109 (2005) 8693.
[22] M.Y. Kuo, Ph.D. Thesis, National Sun Yat-sen University, Taiwan, 2004.
[23] R. Asahi, T. Morikawa, T. Ohwaki, K. Aoki, Y. Taga, Science 293 (2001) 269.
[24] Y. Suda, H. Kawasaki, T. Ueda, T. Ohshima, Thin Solid Films 453–454 (2004) 162.
[25] S.H. Mohamed, O. Kappertz, T. Niemeier, R. Drese, M.M. Wakkad, M. Wuttig, Thin Solid Films 468 (2004) 48.
[26] F.M. Gao, J.L. He, E.D. Wu, S.M. Liu, D.C. Li, S.Y. Zhang, Y.J. Tian, Phys. Rev. Lett. 91 (2003) 015502.
[27] L.S. Dubrovinsky, N.A. Dubrovinskaia, V. Swamy, J. Muscat, N.M. Harrison, R. Ahuja, B. Holm, B. Johansson, Nature 410 (2001) 653.
[28] I.M. Chen, S.W. Yeh, S.Y. Chiou, D. Gan, P. Shen, Thin Solid Films 491 (2005) 339.
[29] S.W. Yeh, T.Y. Hsieh, H.L. Huang, D. Gan, P. Shen, J. Cryst. Growth 289 (2) (2006) 690.